

# Reversible Property Switching, Thermoelectric Performance, and $d^{10}-d^{10}$ Interactions in $\text{Ag}_5\text{Te}_2\text{Cl}$ <sup>†</sup>

Tom Nilges,<sup>\*,†</sup> Oliver Osters,<sup>†</sup> Melanie Bawohl,<sup>†</sup> Jean-Louis Bobet,<sup>‡</sup> Bernard Chevalier,<sup>‡</sup> Rodolphe Decourt,<sup>‡</sup> and Richard Wehrich<sup>§</sup>

<sup>†</sup>Universität Münster, Institut für Anorganische und Analytische Chemie, Corrensstrasse 30, 48149 Münster, Germany, <sup>‡</sup>CNRS, Université de Bordeaux, ICMCB, 87 avenue du Docteur Albert Schweitzer, 33608 Pessac Cedex, France, and <sup>§</sup>Universität Regensburg, Universitätsstrasse 31, 93040 Regensburg, Germany

Received January 27, 2010. Revised Manuscript Received March 26, 2010

Thermoelectric and phase analytical measurements were performed to investigate the physical properties of trimorphic  $\text{Ag}_5\text{Te}_2\text{Cl}$ . The material is a mixed electron/silver ion conductor featuring drastic property changes during a silver order/disorder phase transition at 334 K. The transition is characterized by a jump in the total electric conductivity by 2 orders of magnitude directly affecting the electric and thermoelectric properties. Silver ions are arranged in well-defined strands along the crystallographic  $c$ -axis characterized by a set of not fully occupied sites. Heat capacity measurements show a large effect, whereas the thermopower and thermal diffusivity drop significantly at the temperature of transition. Right after the transition, an attractive  $d^{10}-d^{10}$  interaction within the disordered silver substructure occurs affecting the  $c$ -lattice parameter upon heating. Due to this interaction a modulation of the electronic structure and the thermoelectric properties can be observed which have been investigated in detail. While the thermopower stays low with increasing temperature the thermal diffusivity relaxes fast to values before the transition. At 355 K, the thermopower starts rising again, which is consistent with a small effect in the heat capacity and a reduction of the  $c$ -lattice parameter upon heating. Further heating leads to a reduction of the  $d^{10}-d^{10}$  interactions and a drastic increase in the thermopower. The observed phenomenon must be regarded as a new example of a compound following the recently discovered concept of low-dimensional partially covalent-bonded structure units that can positively influence thermoelectric properties in bulk materials.  $\text{Ag}_5\text{Te}_2\text{Cl}$  is the first example where mobile  $d^{10}$  ions interact to create low-dimensional partially covalent-bonded subunits in a solid, which then leads to a switching of thermoelectric and electronic properties. The system shows very low thermal conductivities between  $0.19 \text{ W m}^{-1} \text{ K}^{-1}$  and  $0.60 \text{ W m}^{-1} \text{ K}^{-1}$  in the temperature range 298 to 500 K, reaching a maximal  $ZT$  value of 0.033 at high temperatures.

## 1. Introduction

A strong demand on new technologies and concepts for the improvement of energy material is present today, which leads to an intensive scientific activity in the field of thermoelectrics.<sup>1–4</sup> A controversial discussion has been initiated dealing with the possible improvement of today's state of the art materials for energy conversion purposes.<sup>5,6</sup>  $ZT$  values ( $ZT$  represents the thermoelectric figure of merit  $Z = S^2\sigma\kappa_{\text{tot}}^{-1}$ , with  $S$  = thermopower,  $\sigma$  = total electric conductivity, and  $\kappa_{\text{tot}}$  = total thermal conductivity) of bulk materials are still too low to be efficiently used in commercial large scale applications. Nanostructured compounds with more interesting values  $ZT > 2$  are not commercially

available at the moment.<sup>7–10</sup> As stated by Sales<sup>11</sup> in a recent article: new concepts and ideas are badly needed to develop a bulk material at low cost and high efficiency by a reduction in  $\kappa_{\text{tot}}$  and improvement in the power factor  $S^2\sigma$ .

Recently, such a new concept for the improvement of thermoelectric and resistivity switching materials was found independently for Peierls-distorted polyanionic Te- and polycationic In-chains in the coinage metal polychalcogenide halide  $\text{Ag}_{10}\text{Te}_4\text{Br}_3$ <sup>12,13</sup> and  $\text{In}_4\text{Se}_{3-\delta}$ .<sup>14</sup>

<sup>†</sup> Dedicated to Prof. Dr. R. Kniep on the occasion of his 65th birthday.  
\*Corresponding author. Phone: +49 (0)251 83 36645. Fax: +49 (0)251 83 36002. E-mail: nilges@uni-muenster.de.  
(1) Snyder, G. J.; Toberer, E. S. *Nat. Mater.* **2008**, 7, 105.  
(2) Kanatzidis, M. G. *Chem. Mater.* **2010**, 22, 648–659.  
(3) Kleinke, H. *Chem. Mater.* **2010**, 22, 604–611.  
(4) Toberer, E. S.; May, A. F.; Snyder, G. J. *Chem. Mater.* **2010**, 22, 624–634.  
(5) Vining, C. B. *Nat. Mater.* **2009**, 8, 83.  
(6) Bell, L. E. *Science* **2008**, 321, 1457.

(7) Hsu, K. F.; Loo, S.; Guo, F.; Chen, W.; Dyck, J. S.; Uher, C.; Hogan, T.; Polychroniadis, E. K.; Kanatzidis, M. G. *Science* **2004**, 303, 818.  
(8) Harman, T. C.; Taylor, P. J.; Spears, D. L.; Walsh, M. P. *J. Electron. Mater.* **2000**, 29, L1.  
(9) Harman, T. C.; Walsh, M. P.; Laforge, B. E.; Turner, G. W. *J. Electron. Mater.* **2005**, 34, L19.  
(10) Venkatasubramanian, R.; Siivola, E.; Colpitts, T.; O'Quinn, B. *Nature* **2001**, 413, 597.  
(11) Sales, B. C. *Int. J. Ceram. Technol.* **2007**, 4, 291.  
(12) Janek, J. *Nat. Mater.* **2009**, 8, 88.  
(13) Nilges, T.; Lange, S.; Bawohl, M.; Deckwart, J.-M.; Wiemhöfer, H.-D.; Decourt, R.; Chevalier, B.; Vannahme, J.; Eckert, H.; Wehrich, R. *Nat. Mater.* **2009**, 8, 101.  
(14) Rhyee, J.-S.; Lee, K. H.; Lee, S. M.; Cho, E.; Kim, S. I.; Lee, E.; Kwon, Y. S.; Shim, J. H.; Kotliar, G. *Nature* **2009**, 459, 965.

First discovered for mobile Te-chains in  $\text{Ag}_{10}\text{Te}_4\text{Br}_3$  this low-dimensional unit creates a modulation of the electronic structure, which results in (i) a *pnp*-switch of the semiconducting properties and (ii) a drastic thermopower drop of about  $1400 \mu\text{V K}^{-1}$  during a structural phase transition.

A Peierls-distorted In-chain is responsible for a huge *ZT* value of 1.48 at 705 K in  $\text{In}_4\text{Se}_{3-\delta}$ . Even materials with switchable properties like resistivity, thermopower or thermal diffusivity, initiated by external stimuli are highly interesting for a significant number of advanced technologies.<sup>15,16</sup> Therefore, the concept of Peierls-chains is not only to be regarded in light of thermoelectrics but also with respect to data storage<sup>17</sup> and sensor applications,<sup>18</sup> and as a key effect during phase transitions.<sup>19,20</sup>

Silver(I) chalcogenide halides like  $\text{Ag}_3\text{SX}$  (with  $X = \text{Br}, \text{I}$ ),<sup>21–23</sup>  $\text{Ag}_5\text{Te}_2\text{Cl}$ ,<sup>24–28</sup> or  $\text{Ag}_{19}\text{Te}_6\text{Br}_7$ ,<sup>29,30</sup> and silver(I) polychalcogenide halides like  $\text{Ag}_{10}\text{Te}_4\text{Br}_3$ ,<sup>31–34</sup>  $\text{Ag}_{23}\text{Te}_{12}\text{X}$  ( $X = \text{Cl}, \text{Br}$ ),<sup>35,36</sup> or  $\text{Ag}_{20}\text{Te}_{10}\text{BrI}$ <sup>37</sup> are mixed conducting materials with a high ion conductivity comparable with related compounds like  $\text{Ag}_7\text{Fe}_3(\text{X}_2\text{O}_7)_4$  with ( $X = \text{P}, \text{As}$ ),<sup>38</sup>  $\text{Ag}_8\text{I}_2(\text{CrO}_4)_3$ ,<sup>39</sup>  $\text{Ag}_4\text{I}_2\text{SeO}_4$ , or  $\text{Ag}_3\text{ITeO}_4$ <sup>40</sup> in this field. Although all the above-mentioned polychalcogenides contain anionic structure units, capable of performing a Peierls-distortion in the solid state, the chalcogenide halides do not fulfill the structural requirements for such a partial covalent bonding in the anion substructure. Anions are well-separated from each other and no tendency of chalcogen for a primary or even secondary interaction, like observed in many other tellurides and

polytellurides,<sup>41</sup> can be found. The above-mentioned concept seemed not to be applicable for the chalcogenide halides so far.

$\text{Ag}_5\text{Te}_2\text{Cl}$  is a trimorphic system with two reversible phase transitions at 240.9(2) and 334.2(5) K.<sup>26</sup> The second transition is accompanied by a jump of the total conductivity of 2 orders of magnitude due to a silver order/disorder phase transition. First discovered<sup>24</sup> in 1985, the complete structure determination of all polymorphs lasted until 2004 due to severe twinning problems and the high mobility of silver within the silver substructure.<sup>25,26</sup> The structure type can be kept over a wide range of different substitutions within the anion substructure. It has been shown that telluride ions can be partially substituted by selenide and sulfide<sup>27,28</sup> ions and chloride can be fully exchanged by bromide or partially substituted by iodide without a change in the realized structure type.<sup>42,43</sup> This feature promises a reasonable chance for property tuning of this class of compounds because of the fact that the transition temperatures of the different polymorphs can be varied over a wide range of temperature by this substitution.

With the discovery of  $\text{Ag}_{10}\text{Te}_4\text{Br}_3$  featuring a linear Peierls-distorted Te-chain and  $\text{In}_4\text{Se}_{3-\delta}$  containing a Peierls distorted In-chain a new concept for the optimization of thermoelectric materials has been postulated. It has been shown that a modulation of the electronic structure can be initiated based on this low-dimensional interactions which can significantly influence the thermopower and thermal diffusivity of these materials. In the case of the silver(I)polychalcogenide halide, this effect came along with a structural phase transition and a mobility of the respective Te-strand at this point. Herein, we will investigate the thermopower and thermal diffusivity evolution of trimorphic  $\text{Ag}_5\text{Te}_2\text{Cl}$  in order to check the possibility of comparable electronic effects after the introduction of mobility to the silver ions during and after the order–disorder phase transition in this compound.

## 2. Experimental Section

**2.1. Synthesis and Phase Analysis.**  $\text{Ag}_5\text{Te}_2\text{Cl}$  was prepared from silver (Chempur, 99.9%), tellurium (Chempur, 99.9%) and silver(I) chloride (Alfa, 99.999%) by reacting a 4:2:1 Ag:Te:AgCl molar mixture in evacuated silica ampules. The starting materials were heated to 1279 K and kept at this temperature for 24 h. After being quenched to room temperature, the crude product was homogenized by grinding in a mortar for 15 min and then annealed at 620 K for 21 days. The purity of the product was checked by X-ray powder phase analysis and EDX-measurements (energy dispersive X-ray spectroscopy, Zeiss Leica 420i scanning electron microscope fitted with an Oxford energy dispersive detector unit; Ag, HgTe (Te), and KCl (Cl) were used as standards for calibration, applying a voltage of 20 kV to the samples) prior to and again after all physicochemical experiments. All samples were phase-pure before and after the measurements.

**2.2. Heat Capacity  $C_p$ .** Finely ground  $\text{Ag}_5\text{Te}_2\text{Cl}$  was pressed to a pellet (107.5 mg) and glued to the platform of a precalibrated

- (15) Terabe, K.; Hasegawa, T.; Nakayama, T.; Aono, M. *Nature* **2005**, 433, 47.
- (16) Waser, R.; Aono, M. *Nat. Mater.* **2007**, 6, 833.
- (17) Huo, M. X.; Li, Y.; Song, Z.; Sun, C. P. *EPL* **2008**, 84, 30004.
- (18) Dürig, U. J. *Appl. Phys.* **2005**, 98, 044906.
- (19) Ovsyannikov, S. V.; Shchennikov, V. V.; Popova, S. V.; Derevskov, A. Yu. *Phys. Status Solidi B* **2003**, 235, 521.
- (20) Sciaini, G.; Harb, M.; Kruglik, S. G.; Payer, T.; Hebeisen, C. T.; Meyer zu Heringdorf, F.-J.; Yamaguchi, M.; Horn von Hoegen, M.; Ernstorfer, R.; Dwayne Miller, R. J. *Nature* **2009**, 458, 56.
- (21) Reuter, B.; Hardel, K. *Naturwissenschaften* **1961**, 48, 161.
- (22) Reuter, B.; Hardel, K. Z. *Anorg. Allg. Chem.* **1965**, 340, 168.
- (23) Hull, S.; Keen, D. A.; Gardner, N. J.G.; Hayes, W. J. *Phys.: Condens. Matter* **2001**, 13, 2295.
- (24) Blachnik, R.; Dreisbach, H. J. *Solid State Chem.* **1985**, 60, 115.
- (25) Doert, T.; Rönsch, E.; Schnieders, F.; Böttcher, P.; Sieler, J. Z. *Anorg. Allg. Chem.* **2000**, 626, 89.
- (26) Nilges, T.; Nilges, S.; Pfitzner, A.; Doert, T.; Böttcher, P. *Chem. Mater.* **2004**, 16, 806.
- (27) Nilges, T.; Dreher, C.; Hezinger, A. *Solid State Sci.* **2005**, 7, 79.
- (28) Nilges, T.; Lange, S. Z. *Anorg. Allg. Chem.* **2005**, 631, 3002.
- (29) Nilges, T.; Messel, J.; Bawohl, M.; Lange, S. *Chem. Mater.* **2008**, 20, 4080.
- (30) Nilges, T.; Messel, J. Z. *Anorg. Allg. Chem.* **2008**, 634, 2185.
- (31) Lange, S.; Nilges, T. *Chem. Mater.* **2006**, 18, 2538.
- (32) Lange, S.; Bawohl, M.; Wilmer, D.; Meyer, H.-W.; Wiemhöfer, H.-D.; Nilges, T. *Chem. Mater.* **2007**, 19, 1401.
- (33) Nilges, T.; Bawohl, M.; Lange, S. Z. *Naturforsch.* **2007**, 62b, 955.
- (34) Nilges, T.; Bawohl, M. Z. *Naturforsch.* **2008**, 63b, 629.
- (35) Lange, S.; Bawohl, M.; Nilges, T. *Inorg. Chem.* **2008**, 47, 2625.
- (36) Osters, O.; Nilges, T. Z. *Anorg. Allg. Chem.* **2010**, 636, 297–304.
- (37) Nilges, T.; Bawohl, M.; Lange, S.; Messel, J.; Osters, O. J. *Electron. Mater.* **2010**, DOI: 10.1007/s11664-009-0987-9.
- (38) Quarez, E.; Mentré, O.; Oumellala, Y.; Masqueliera, C. *New J. Chem.* **2009**, 33, 998.
- (39) Pitzschke, D.; Curda, J.; Jansen, M. Z. *Anorg. Allg. Chem.* **2009**, 635, 926.
- (40) Pitzschke, D.; Curda, J.; Cakmak, G.; Jansen, M. Z. *Anorg. Allg. Chem.* **2008**, 634, 1071.
- (41) Graf, C.; Assoud, A.; Mayasree, O.; Kleinke, H. *Molecules* **2009**, 14, 3115.

(42) Messel, J.; Nilges, T. Z. *Naturforsch.* **2008**, 63b, 1077.

(43) Bawohl, M.; Nilges, T. Z. *Naturforsch.* **2008**, 63b, 1083.

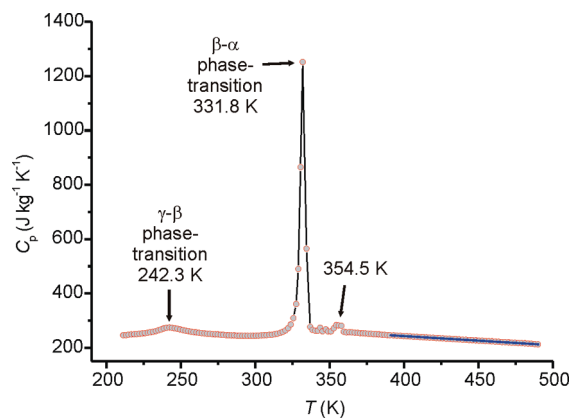


**Figure 1.** Measured heat capacity  $C_p$  in  $\text{J kg}^{-1} \text{K}^{-1}$  of  $\text{Ag}_5\text{Te}_2\text{Cl}$ . The first two effects correspond to the reported phase transitions at 240.9(2) and 334.2(5) K (data from<sup>26</sup>). A third new effect was found at 354.5 K. The blue line denotes extrapolated values up to 490 K.

heat capacity puck of a Quantum design physical property measurement system (PPMS).  $C_p$  measurements have been performed using the  $C_p$  option of the PPMS in the temperature range from 210 to 390 K (Figure 1).

**2.3. Thermal Diffusivity  $a$ .** Powdered  $\text{Ag}_5\text{Te}_2\text{Cl}$  was pressed to pellets of 6 mm in diameter and 11 or 18 mm thickness reaching a value of >98% of the theoretical X-ray density. Independent measurements were performed for each pellet covering the temperature range of 293 to 473 K. All data are summarized in the Supporting Information and Figure 3. The thermal diffusivity was measured by a commercial Netzsch Laser Microflash apparatus in a SiC sample holder under Ar-atmosphere. Five independent shots were performed and averaged for each data point in the temperature range of 293–473 K. The thermal diffusivity was derived from the raw data using the Proteus software package.

**2.4. Thermopower  $S$ .** A  $\text{Ag}_5\text{Te}_2\text{Cl}$  pellet of 6 mm diameter and 18 mm thickness (the same as used for thermal diffusivity measurements) was transferred to a homemade thermopower machine and data were determined in the temperature range of 308 to 500 K. The thermopower measurements were carried out using a dynamic method (constant heating during the measurement, detection of the cell voltage versus time; accuracy of the thermopower within  $\pm 1\%$ ), suitable for high-resistivity samples as well as metals featuring a thermopower lower than  $10 \mu\text{V K}^{-1}$ . Details of the cell and measurement methods are described elsewhere.<sup>44</sup>

**2.5. Temperature-Dependent X-ray Powder Diffraction.** Temperature-dependent X-ray powder diffraction was performed in a temperature range from 298 to 393 K using a Stoe STADI P diffractometer fitted with  $\text{Mo K}\alpha$  radiation ( $\lambda = 0.71073 \text{ \AA}$ ) and a curved  $130^\circ$  Stoe image plate detector. A powdered sample of  $\text{Ag}_5\text{Te}_2\text{Cl}$  was mixed with amorphous powdered silica glass in a volumetric 1:1 ratio under an Ar-atmosphere and was transferred to a 0.3 mm silica glass capillary. The capillary was then sealed with grease at the top and mounted to a Stoe heating unit capable to control the temperature within  $\pm 0.5 \text{ K}$ . Data were collected for 12 h for each data set at various temperatures. A cell refinement was performed for each data set using the Stoe Win-Xpow program suite.<sup>45</sup>

**2.6. Single-Crystal X-ray Diffraction.** A single crystal of suitable size for structure determination was isolated from the

final reaction batch after the melting and annealing process. It was transferred to a silica tube which was evacuated and refilled with  $\text{N}_2$  prior to the data collection on a Stoe IPDSII diffractometer ( $\text{Mo K}\alpha$  radiation;  $\lambda = 0.71073 \text{ \AA}$ ). Data were collected for  $\beta\text{-Ag}_5\text{Te}_2\text{Cl}$  at 300 K and after the order/disorder transition for  $\alpha\text{-Ag}_5\text{Te}_2\text{Cl}$  between 343.1 and 433.1 K (one data set every 10 K). The temperature was controlled by a Cryostream plus system (Oxford) with an accuracy of the absolute temperature of  $\pm 0.5 \text{ K}$  and a temperature stability of  $\pm 0.1 \text{ K}$  during the data collection. A numerical absorption correction<sup>46</sup> was performed independently for each data set based on an optimized crystal shape derived from the symmetry equivalent reflections. The structure refinements<sup>47</sup> were based on the previously reported structure models for the  $\beta$ - and  $\alpha\text{-Ag}_5\text{Te}_2\text{Cl}$  phase using non-harmonic displacement parameters up to the third order for the description of the silver ion distribution. All silver mode positions are derived from the maxima of electron density and are used for a discussion of the average silver ion distances within the silver substructure. A detailed procedure for the structure refinement of compounds featuring high ion mobility in the solid state is given elsewhere.<sup>26</sup>

**2.7. Thermal Conductivity  $\kappa_{\text{tot}}$  and Figure of Merit  $ZT$ .** The thermal conductivity was calculated by the following equation

$$\kappa_{\text{tot}} = a\rho C_p \quad (1)$$

using the measured heat capacity  $C_p$ , the measured thermal diffusivity  $a$  and the density  $\rho$ . The density was extrapolated from the measured X-ray density of four single-crystal structure analyses at 298, 373, 423, and 453 K (see the literature<sup>26</sup>). The extrapolated values (data in the Supporting Information) are consistent with the calculated densities from the temperature-dependent X-ray powder phase analyses.

$ZT$  values are calculated by following equation

$$ZT = \frac{S^2\sigma}{\kappa_{\text{tot}}}T \quad (2)$$

with the measured thermopower  $S$ , the total electric conductivity  $\sigma$  taken from literature<sup>26</sup> and the calculated total thermal conductivity  $\kappa_{\text{tot}}$ . All data are summarized in the Supporting Information.

**2.8. DFT Calculations.** The calculations of isolated Ag strands were performed with the LCAO code of CRYSTAL06,<sup>48</sup> applying DFT-GGA and LDA exchange and correlation functionals.<sup>49</sup> A small core *Hay-Wadt* type valence basis set was used for Ag to calculate the electronic structures and total energy values.<sup>50</sup> Therein, the Ag-4s, 4p, 4d, 5s, and 5p orbitals are treated as valence states, inner electrons are described as core states. The  $\text{Ag}^+-\text{Ag}^+$  interactions were calculated within model structures varying distances within chains of 2, 3, and 4  $\text{Ag}^+$  ions. Basis set performance was tested at HW-311d1G level applying coefficients for outer basis set functions as 0.15 (sp) and 0.2 (d). At the HWSC-311d1G level a further sp

(46) *Stoe Xred and X-shape*, Ver. 1.48 and Ver. 2.11; Stoe & Cie GmbH: Darmstadt, Germany, 2008.

(47) Petricek, V.; Dusek, M.; Palatinus, L. *Jana2006 The Crystallographic Computing System*; Institute of Physics: Praha, Czech Republic, 2006.

(48) Dovesi, R.; Saunders, V. R.; Roetti, C.; Orlando, R.; Zicovich-Wilson, C. M.; Pascale, F.; Civalieri, B.; Doll, K.; Harrison, N. M.; Bush, I. J.; D'Arco, Ph.; Llunell, M. *CRYSTAL06 User'S Manual*; University of Torino: Torino, Italy, 2006; www.crystal.unito.it

(49) Perdew, J. P.; Burke, K.; Ernzerhof, M. *Phys. Rev. Lett.* **1996**, *77*, 3865. Vosko, S. H.; Wilk, L.; Nusair, M. *Can. J. Phys.* **1980**, *58*, 1200.

(50) Apra, E.; Stefanovich, E.; Dovesi, R.; Roetti, C. *Chem. Phys. Lett.* **1991**, *186*, 329.

(44) Dordor, P.; Marquestaut, E.; Villeneuve, G. *Rev. Phys. Appl.* **1980**, *15*, 1607.

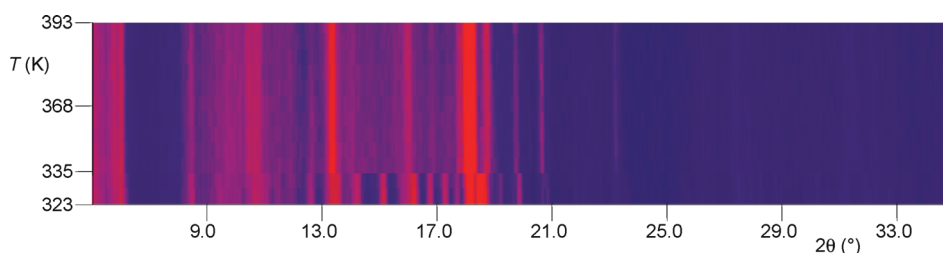
(45) *Stoe Xpow*, Ver. 1.2; Stoe & Cie GmbH: Darmstadt, Germany, 2001.



Table 1. Crystallographic Data from Temperature-Dependent X-ray Powder Diffraction of  $\text{Ag}_5\text{Te}_2\text{Cl}$  between 298 and 393 K<sup>a</sup>

phase	<i>T</i> (K)	<i>a</i> (Å)	<i>b</i> (Å)	<i>c</i> (Å)	$\beta$ (deg)	<i>V</i> (Å <sup>3</sup> )	<i>Z</i>	<i>V</i> <sub>FU</sub> (Å <sup>3</sup> )
$\beta$	303	13.837(14)	7.62(3)	13.624(13)	90.25(6)	1436.8(51)	8	179.6
$\beta$	313	13.854(9)	7.636(11)	13.643(11)	90.26(4)	1443.3(33)	8	180.4125
$\beta$	323	13.916(3)	7.6366(25)	13.6168(22)	90.371(9)	1447.0(5)	8	180.875
$\beta$	333	13.902(14)	7.650(9)	13.696(13)	90.33(5)	1456.5(24)	8	182.0625
$\alpha$	348	9.734(5)		7.831(6)		742.0(6)	4	185.5
$\alpha$	353	9.753(9)		7.848(8)		746.6(16)	4	186.65
$\alpha$	358	9.749(9)		7.841(7)		745.2(14)	4	186.3
$\alpha$	363	9.754(18)		7.859(15)		747.8(31)	4	186.95
$\alpha$	368	9.769(12)		7.859(12)		750.0(23)	4	187.5
$\alpha$	373	9.787(11)		7.885(7)		755.3(15)	4	188.825
$\alpha$	378	9.785(6)		7.875(9)		754.0(6)	4	188.5
$\alpha$	383	9.798(10)		7.879(10)		756.4(18)	4	189.1
$\alpha$	388	9.779(10)		7.868(9)		752.5(18)	4	188.125
$\alpha$	393	9.788(13)		7.874(11)		754.5(23)	4	188.625

<sup>a</sup> Mo  $K_{\alpha}$  radiation ( $\lambda = 0.71073$  Å); *FU* = formula unit; *Z* = *FU* per cell;  $\beta$ -phase monoclinic,  $P2_1/n$ ;  $\alpha$ -phase tetragonal,  $I4/mcm$ .



**Figure 2.** Temperature-dependent X-ray powder diffraction experiment of  $\text{Ag}_5\text{Te}_2\text{Cl}$  in the temperature range 323–393 K. The  $\beta$ – $\alpha$  phase transition occurs at  $\sim 335$  K. No obvious additional transition can be observed above 335 K. Crystallographic data are summarized in Table 1.

shell and all outer shell parameters were optimized (sp: 0.0336, 0.1699, d: 0.2166). A model cell was used to account for nearest  $\text{Ag}^+$ – $\text{Ag}^+$  interactions within pairs and to single  $\text{Ag}^+$  ions as next nearest neighbors as found within the chains. Therefore, total energy and electronic structure calculations were performed first for isolated  $\text{Ag}^+$ – $\text{Ag}^+$  pairs changing the atomic distances within the pairs, whereas the distances to next pairs remained more than 5 Å. Second, additional interactions to neighboring  $\text{Ag}^+$  ions along and beside the pairs were considered to account for possible bonding situations within the helical chains of  $\text{Ag}^+$  ions found experimentally.

### 3. Results and Discussion

$\text{Ag}_5\text{Te}_2\text{Cl}$  represents a mixed conducting compound<sup>51</sup> on the quasi-binary section  $\text{Ag}_2\text{Te}$ – $\text{AgCl}$ <sup>24</sup> and is described as a trimorphic system with two reversible phase transitions at 240.9(2) K ( $\gamma$ – $\beta$  transition) and 334.2(5) K ( $\beta$ – $\alpha$  transition).<sup>26</sup> The first transition is characterized by a small dislocation of the cations and anions, which causes a doubling of the unit-cell volume from room to deep temperature phase. From the heat capacity measurement, this transition can be identified as a small effect with a peak maximum at 242.3 K (Figure 1). A huge  $\lambda$ -shaped effect in the  $C_p$  curve comes along with the second phase transition at 331.8 K featuring a heat capacity maximum of 1252.5 J kg<sup>−1</sup> K<sup>−1</sup>. Surprisingly, a small third effect with an  $C_p$  maximum of 283.7 J kg<sup>−1</sup> K<sup>−1</sup> can be observed at 354.5 K which has not been reported before in literature.

The total electrical conductivity<sup>26</sup> shows a sharp increase of about 2 orders of magnitude at the  $\beta$ – $\alpha$  transition (see the Supporting Information), but no deviation from an Arrhenius-type behavior above this temperature. Around 355 K, a continuous increase in the total conductivity is present giving no hint for a modulation of the electric properties at this temperature. To check the occurrence of a fourth polymorph in the temperature range 334–355 K, we performed a detailed temperature dependent X-ray powder diffraction analysis covering the temperature range 298–393 K. Table 1 and Figure 2 summarize the results from these phase analytic experiments. All diffractograms could either be indexed with the  $\beta$ -type (298–323 K) or the  $\alpha$ -type structure and we found no hint for a structural phase transition around 355 K. At least the space group type remains the same. Additional single-crystal structure determinations were done at 300 and between 343 and 433 K in steps of 10 K substantiating this general finding. A selection of crystallographic data and bond length is given in Tables S3–S5 in the Supporting Information, respectively.

To verify the thermoelectric properties of  $\text{Ag}_5\text{Te}_2\text{Cl}$ , a detailed examination of the thermopower and the thermal diffusivity was performed. Surprisingly,  $\text{Ag}_5\text{Te}_2\text{Cl}$  shows the same thermopower characteristics as was observed in the case of the silver(I) polychalcogenide halide  $\text{Ag}_{10}\text{Te}_4\text{Br}_3$ . A significant drop of the thermopower occurs from 397  $\mu\text{V K}^{-1}$  at 316 K (Figure 3), right before the transition to 105  $\mu\text{V K}^{-1}$  at 333.9 K, representing the exact point of transition. In the following, the thermopower stays relatively low between 146 and 91  $\mu\text{V K}^{-1}$ , up to 359 K, where it starts raising again to a maximal value of 573  $\mu\text{V K}^{-1}$  at 441 K. This drop is

(51) Beeken, R. B.; Wang, S. M.; Smith, D. R. *Solid State Ionics* **1992**, 53–56, 220.

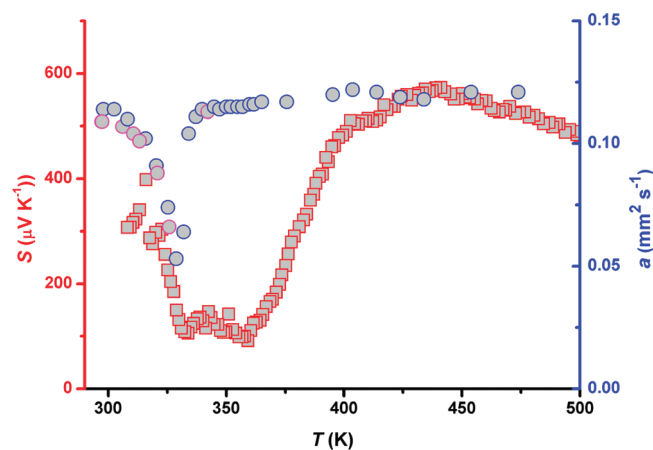


**Figure 3.** Measured thermal diffusivity (two independent measurements)  $a$  in  $\text{mm}^2 \text{s}^{-1}$  (right axis) and thermopower  $S$  in  $\mu\text{V K}^{-1}$  (left axis) in the temperature range of 290–500 K. The huge drop in the thermopower and thermal diffusivity is consistent with the  $\beta$ – $\alpha$  order/disorder phase transition of  $\text{Ag}_5\text{Te}_2\text{Cl}$ . Although the thermal diffusivity equilibrates fast from the minimal value of  $0.053 \text{ mm}^2 \text{s}^{-1}$  at 329 K to values before the phase transition, a broad thermopower effect remains present after the phase transition. The thermopower stays low and slightly decreases down to  $91 \mu\text{V K}^{-1}$  at 359 K before it raises again to a maximal value of  $573 \mu\text{V K}^{-1}$  at 441 K.

consistent with the findings for  $\text{Ag}_{10}\text{Te}_4\text{Br}_3$  and  $\text{In}_4\text{Se}_{3-\delta}$ , where a Peierls-distorted chain of either partially covalent-bonded Te or In was responsible for a strong modulation of the electronic structure and the performance of the thermoelectric properties. In contrast to the previous examples, a plateau regime of the thermopower with almost constant values after the drop represents the major difference between  $\text{Ag}_5\text{Te}_2\text{Cl}$  and the two Peierls systems. The absolute thermopower of  $\text{Ag}_5\text{Te}_2\text{Cl}$  stays positive over the whole temperature range under investigation indicating a  $p$ -type (hole) conduction.

Surprisingly, the thermal diffusivity is low and covers a range of  $0.11$  to  $0.12 \text{ mm}^2 \text{s}^{-1}$  over a temperature range of 298 to 473 K (Figure 3). These values are comparable with room temperature values of isolators like poly(ethylene terephthalate) ( $0.16 \text{ mm}^2 \text{s}^{-1}$ ),<sup>52</sup> polytetrafluoroethylene ( $0.10 \text{ mm}^2 \text{s}^{-1}$ ),<sup>53</sup> or low density polyethylene ( $0.18 \text{ mm}^2 \text{s}^{-1}$ ).<sup>54</sup> At the  $\beta$ – $\alpha$  phase transition a significant reduction of the thermal diffusivity to a very low value of  $0.053 \text{ mm}^2 \text{s}^{-1}$  at 329 K occurs that substantiated the huge mobility of the silver cations and the rearrangement of the anions during the transition.

In contrast to the polychalcogenide halide  $\text{Ag}_{10}\text{Te}_4\text{Br}_3$ , the chalcogenide halide  $\text{Ag}_5\text{Te}_2\text{Cl}$  can not undergo any covalent interaction within the anion substructure and therefore no Peierls-like distortion can take place. We found no hints for any local mobility of the two nuclei  $^{35}\text{Cl}$  and  $^{125}\text{Te}$  by NMR spectroscopic investigations within the different polymorphs.<sup>55</sup> This changes completely for the silver cations. Even for the low temperature  $\gamma$ -phase a

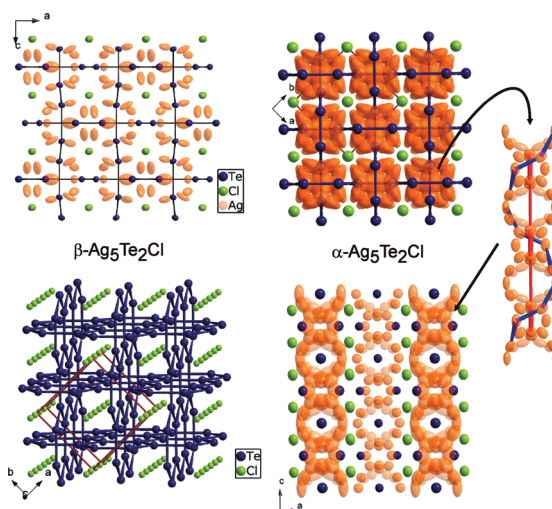


**Figure 4.** Crystal structure sections of  $\beta$ - $\text{Ag}_5\text{Te}_2\text{Cl}$  (298 K) and  $\alpha$ - $\text{Ag}_5\text{Te}_2\text{Cl}$  (573 K). The silver ions are forming a strand of delocalized silver along the  $c$ -axis in  $\alpha$ - $\text{Ag}_5\text{Te}_2\text{Cl}$ . Two different models for a  $d^{10}$ – $d^{10}$  interaction within the strands are given.

certain forward–backward hopping of silver ions is present on the millisecond scale and the ion mobility increases with increasing temperature and the type of polymorph. A pronounced silver mobility and exchange on different positions could be derived from static and MAS-<sup>109</sup>Ag NMR data. Activation energies from NMR data<sup>55</sup> (and dc-conductivity data<sup>26</sup>) are 0.19 eV (0.14 eV) for  $\alpha$ - $\text{Ag}_5\text{Te}_2\text{Cl}$  and 0.38 eV (0.44 eV) for the  $\beta$ -phase, respectively. A pronounced one-dimensional arrangement of disordered and mobile silver along the crystallographic  $c$ -axis is created where silver is distributed over a wide range of positions (Figure 4).

Exactly in this part of the silver substructure, it is possible to generate such attractive and low dimensional interaction which is capable to tune the thermoelectric features. A direct hint for such interaction is the evaluation of the  $c$ -lattice parameter during heating, as shown in comparison to the thermopower in Figure 5.

Although the  $a$ -axis shows an almost linear increase without any unexpected trend during heating, the  $c$ -lattice parameter seems to decrease on increasing the temperature. Such behavior can be explained by the occurrence of attractive interactions along the  $c$ -axis which should affect the lattice parameter in the present manner. One can expect an anomaly or even a shrinking of the parameter upon heating, which can not be explained without an attractive bonding interaction. For supercooled liquid tellurium, a negative thermal expansion coefficient was found which could be related to the occurrence of a Peierls distorted arrangement of Te chains.<sup>56</sup> In  $\text{Ag}_5\text{Te}_2\text{Cl}$ , the silver substructure is quasi-molten and a comparable situation with the formation of attractive interactions can be expected as for the liquid Te phase. Nevertheless, the trend of the lattice parameter derived from X-ray powder experiments should not be over interpreted because the overall change is not very high and the standard deviations for each value has to be taken into

(52) Morikawa, J.; Hashimoto, T. *Polymer* **1997**, *38*, 5397.

(53) Boudennel, A.; Ibos, L.; Gehin, E.; Candau, Y. *J. Phys. D: Appl. Phys.* **2004**, *37*, 132.

(54) Cella, N.; Vargas, H.; Galembeck, E.; Galembeck, F.; Miranda, L. C. M. *J. Polym. Sci., Part C: Polym. Lett.* **1989**, *27*, 313.

(55) Brinkmann, C.; Faske, S.; Vogel, M.; Nilges, T.; Heuer, A.; Eckert, H. *Phys. Chem. Chem. Phys.* **2006**, *8*, 369.

(56) Zhao, G.; Wu, Y. N. *Phys. Rev. B* **2009**, *79*, 184203.

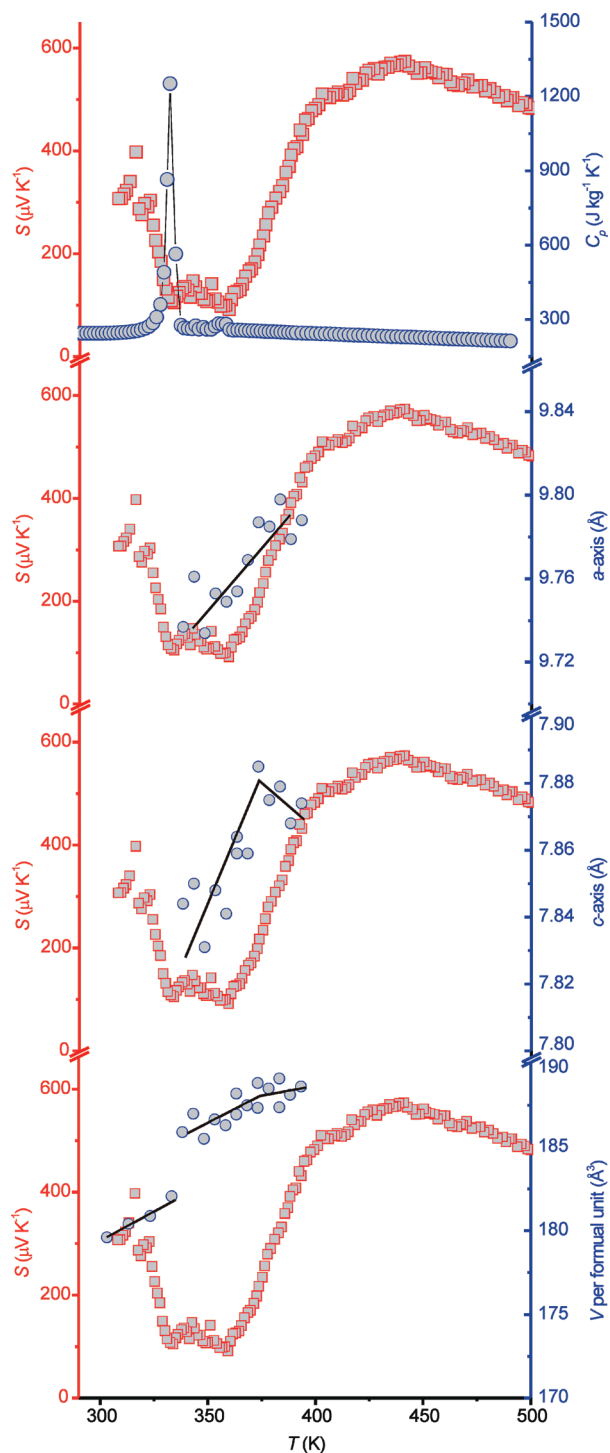


**Figure 5.** Comparison of the thermopower (red squares, left axis),  $C_p$  (blue large circles, right upper axis), and the measured lattice parameters (blue small circles, right middle and bottom axis) of  $\text{Ag}_5\text{Te}_2\text{Cl}$  around the  $\beta$ - $\alpha$  phase transition. A large drop of the thermopower occurs at the phase transition followed by less pronounced reduction up to 355 K. The small effect in the heat capacity at 355 K is consistent with the drastic increase of the thermopower after this temperature. From the temperature-dependent X-ray powder diffraction studies of  $\text{Ag}_5\text{Te}_2\text{Cl}$ , a slight trend in the reduction of the  $c$ -axis (and therefore also the volume per formula unit  $V_{\text{FU}}$ ) can be estimated.

account (see Table 1). We have postulated two possible mechanisms for such an attractive interaction in Figure 4, which both can be the origin of such an effect. Both mechanisms, a interaction within the helical strands (blue

line in the structure section in Figure 4) or a linear arrangement (red line in Figure 4) through the silver chains, involve Ag–Ag distances between 2.9 and 3.2 Å. These intrastrand distances cover the usual range of silver compounds featuring  $d^{10}$ – $d^{10}$  interactions.<sup>57</sup>

To substantiate these mechanisms and the attractive Ag–Ag interactions, we performed a more detailed examination of the silver substructure and the silver distribution in the  $\alpha$ -phase using temperature dependent single-crystal structure determinations. Details of the structure determinations and selected crystallographic data are given in the Supporting Information and can be derived from the Fachinformationszentrum Karlsruhe on quoting the depository numbers CSD 421399 (300 K,  $\beta$ - $\text{Ag}_5\text{Te}_2\text{Cl}$ ), CSD 421400 (343.1 K,  $\alpha$ - $\text{Ag}_5\text{Te}_2\text{Cl}$ ), CSD 421401 (353.1 K,  $\alpha$ - $\text{Ag}_5\text{Te}_2\text{Cl}$ ), CSD 421402 (363.1 K,  $\alpha$ - $\text{Ag}_5\text{Te}_2\text{Cl}$ ), CSD 421403 (373.1 K,  $\alpha$ - $\text{Ag}_5\text{Te}_2\text{Cl}$ ), CSD 421404 (383.1 K,  $\alpha$ - $\text{Ag}_5\text{Te}_2\text{Cl}$ ), CSD 421405 (393.1 K,  $\alpha$ - $\text{Ag}_5\text{Te}_2\text{Cl}$ ), CSD 421406 (403.1 K,  $\alpha$ - $\text{Ag}_5\text{Te}_2\text{Cl}$ ), CSD 421407 (413.1 K,  $\alpha$ - $\text{Ag}_5\text{Te}_2\text{Cl}$ ), CSD 421408 (423.1 K,  $\alpha$ - $\text{Ag}_5\text{Te}_2\text{Cl}$ ), or CSD 421409 (433.1 K,  $\alpha$ - $\text{Ag}_5\text{Te}_2\text{Cl}$ ). The silver distribution within the linear strands in  $\alpha$ - $\text{Ag}_5\text{Te}_2\text{Cl}$  was determined by a nonharmonic description of the silver displacements and a detailed probability density function (pdf) analysis afterward. Mode positions (suffix m), representing the maxima of electron density, have been extracted from the pdf analyses. They represent the positions of highest probability to find a silver ion the mobile silver substructure and were therefore taken into account to discuss Ag–Ag distances in more detail. A full listing of all mode positions is given in the Supporting Information. Figure 6 shows the evolution of the  $\text{Ag}_m$ – $\text{Ag}_m$  distances based on these mode positions with temperature for  $\alpha$ - $\text{Ag}_5\text{Te}_2\text{Cl}$ . For both postulated mechanisms the helical ( $\text{Ag}_{1m}$ – $\text{Ag}_{2m}$  and  $\text{Ag}_{2m}$ – $\text{Ag}_{3m}$ ) and the linear one ( $\text{Ag}_{4m}$ – $\text{Ag}_{4m}$ ) a significant decrease of the Ag–Ag distances starts between 360 and 375 K, in good accordance with the decrease in the  $c$ -lattice parameter derived from powder X-ray analyses at about 375 K (see Figure 5).

Of course, the postulated interactions can not be formed on a large translational section within the silver strand because the occupancy factors of each silver position are lower than 1. Therefore, the formation of a continuous helical silver subunit or Peierls-chain can not be realized and only parts within the postulated strand can interact attractively. The smallest  $\text{Ag}_m$ – $\text{Ag}_m$  distances are localized in the helical arrangement, which is the origin of the strongest interactions. This is a major difference compared to the situations in  $\text{Ag}_{10}\text{Te}_4\text{Br}_3$  and  $\text{In}_4\text{Se}_{3-\delta}$ , where a fully translative and linear Peierls-distorted Te- or In-chain (fully occupied positions within the chain) is responsible for a strong electronic structure and thermopower modulation. In  $\text{Ag}_5\text{Te}_2\text{Cl}$  the formation of simple ion pairs within the helical pathway seems to be the most probable unit to be formed due to the occupancy factors between 0.33 and 0.11 for each silver position (see Table S5 in the Supporting

(57) Jansen, M. *Angew. Chem., Int. Ed.* **1987**, 26, 1098.



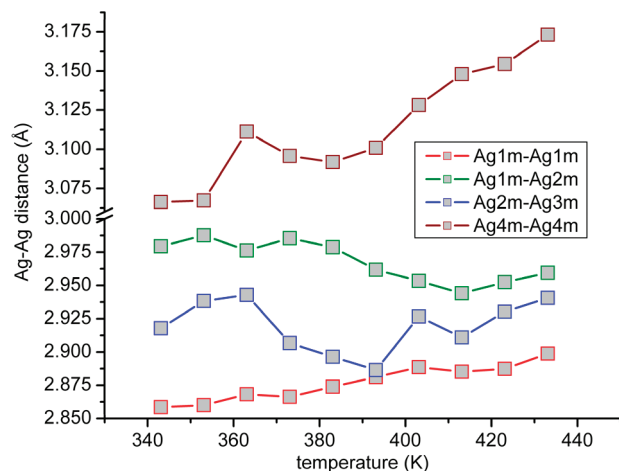


**Figure 6.** Distances (Å) between the silver mode positions (suffix m) in  $\alpha$ -Ag<sub>5</sub>Te<sub>2</sub>Cl. Estimated standard deviations are within the size of the squares. Ag1m–Ag1m represents the interstrand distance between two neighbored silver strands along the *c*-axis. Ag1m–Ag2m and Ag2m–Ag3m are two alternative intrastrand type helical structure sections (see blue line in Figure 4) within the silver strands and Ag4m–Ag4m denotes the linear Peierls-like chain arrangement (red line in Figure 4). A shortening of the Ag–Ag distances starts between 360 and 375 K in the case of all intrastrand distances Ag1m–Ag2m, Ag2m–Ag3m, and Ag4m–Ag4m, whereas the interstrand distance Ag1m–Ag1m increases linearly with temperature.

Information). It is hard or even impossible to decide which of the two effects is more probable because the averaging diffraction methods as well as the local probes like NMR spectroscopy do not resolve the highly dynamic situation in the silver strands properly. Nevertheless, it has been shown in literature for partially covalent-bonded (Peierls-distorted) Sb or Te chains that such covalent interactions can cause a well-defined modulation of the electronic structure from a metallic character and a closed band gap for an equidistant chain toward a semiconducting character with an open band gap for the Peierls-distorted arrangement.<sup>58,13</sup> For instance, the combination of mobile cations and the mobility of atoms within Peierls-chains in Ag<sub>10</sub>Te<sub>4</sub>Br<sub>3</sub> causes a significant drop in thermopower and thermal diffusivity, resulting in a complete switch of the semiconducting properties from p-type via n-type and back to p-type conductivity. A comparable p–n transition caused by attractive Te–Te interactions was observed for the polytelluride {[Ga(en)<sub>3</sub>]<sub>2</sub>(Ge<sub>2</sub>Te<sub>15</sub>)}<sub>n</sub>.<sup>59</sup> We interpret the effect in the heat capacity and the increase in the thermopower between 355 and 359 K as the starting point of the formation of attractive interactions within the silver substructure. This process is followed by a continuous reduction in the covalent interactions that occur with increasing temperature. From the temperature-dependent X-ray powder diffraction experiments within this temperature range, it becomes obvious that the normal thermal expansion of the lattice parameters with increasing temperature is compensated by a positive interaction along the *c*-axis, which obviously results in a slight shortening of the *c*-lattice parameter and some Ag–Ag distances within the silver

strands. At 360 K, the Ag2m–Ag3m distance drops significantly with increasing temperature, consistent with the starting point of the evolution of attractive interactions within the silver substructure along the helical arrangement within the silver strands. We therefore interpret the effect in *C<sub>p</sub>* as the point where the abrupt formation of silver interactions takes place. In contrast to previously reported compounds Ag<sub>10</sub>Te<sub>4</sub>Br<sub>3</sub> and In<sub>4</sub>Se<sub>3–δ</sub> with attractive low-dimensional interactions within linear Peierls-distorted chains the helical path represents the region featuring the most intense attractive interactions in Ag<sub>5</sub>Te<sub>2</sub>Cl. For instance, the Ag2m–Ag3m distance drops from 2.94 Å at 353 K to 2.89 Å at 393 K before it increases again to 2.94 Å at 433 K. This path seems therefore to be the most important feature for the electronic structure modulation necessary to explain the thermopower behavior in the title compound.

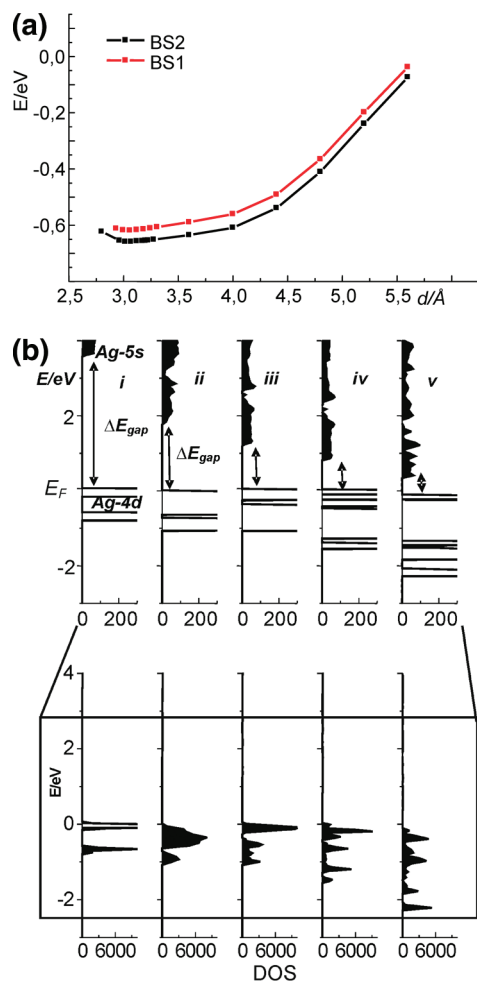
Thermopower modulation can be achieved by a significant change in the density of states near the Fermi level that is influenced by both, nearest, and next nearest Ag<sup>+</sup>–Ag<sup>+</sup> distances. To show the influence of attractive interactions and close Ag<sup>+</sup>–Ag<sup>+</sup> contacts within the silver substructure model DFT (GGA) calculations were performed based on the isolated silver substructure only. Total energy calculations clearly indicate a distortion of isolated Ag<sup>+</sup> ions toward the formation of (Ag<sup>+</sup>)<sub>2</sub> pairs. From LDA calculations Ag<sup>+</sup>–Ag<sup>+</sup> distances of 3.0 and 2.8 Å (Figure 7a) are predicted for isolated ion pairs, and pairs neighbored by single Ag<sup>+</sup> ions (*d* = 3.5 Å), respectively.

Figure 7b shows changes in both the electronic structure related to Ag<sup>+</sup>-dynamics for both valence and conduction band assuming next nearest Ag<sup>+</sup> ions situated 3.5 Å to the Ag<sup>+</sup>–Ag<sup>+</sup> pairs. Similar situations are concluded from the experimental structure within the helical Ag<sup>+</sup> arrangement (see Figure 4). From the analyses of the electronic density of states, one must conclude that Ag<sup>+</sup>–Ag<sup>+</sup> ion pair formation mainly causes the broadening of the Ag-4d states that form the valence band. The broadening of the conduction band and its lowering in energy is additionally supported by next nearest Ag<sup>+</sup> ions (for isolated ion pairs the gap is larger than 2 eV). Total energy calculations also indicate that these neighboring ions drive the Ag<sup>+</sup> dynamics. Assuming ion distances within the pair of more than 3.8 Å the gap between occupied 4d states and unoccupied 5s orbitals is larger than 3 eV (i). Going toward distances of 3.5 Å (ii), the gap is lowered to 1.8 eV. An even closer Ag<sup>+</sup>–Ag<sup>+</sup> distance causes a gap of 1.2 eV (3.0 Å, iii), 0.8 eV (2.8 Å, iv), and 0.5 eV (2.6 Å, v). This can be explained by a combination of both broadening of Ag-4d and a lowering of Ag-5s states due to Ag<sup>+</sup>–Ag<sup>+</sup> interactions. It becomes evident that a formation of interaction causes a pronounced variation of the DOS near the Fermi level, which must account for the change in thermopower.

A density anomaly, with an increase in the measured density with temperature, was found at 353.1 K. The respective densities at 343.1 and 363.1 K of  $\alpha$ -Ag<sub>5</sub>Te<sub>2</sub>Cl are slightly lower than the one at 353.1 and a continuous decrease can be observed upon further heating above

(58) Papoian, G. A.; Hoffmann, R. *Angew. Chem.* **2000**, *112*, 2500.

(59) Zhang, Q.; Malliakas, C. D.; Kanatzidis, M. G. *Inorg. Chem.* **2009**, *48*, 10910.



**Figure 7.** (a) DFT total energy calculations with respect to  $\text{Ag}^+-\text{Ag}^+$  distances within ion pairs. Results are shown for both basis sets BS1 (HWS-311d31G) and BS2 (HWS-311d31G). (b) Results from DFT (GGA) calculations for the isolated silver substructure in  $\text{Ag}_5\text{Te}_2\text{Cl}$ . An enlarged section of the results is given in the upper part pointing out the gap between (occupied) Ag-4d and (unoccupied) Ag-5s states. Ag-Ag pair formation was assumed within silver strands featuring nearest Ag-Ag distances of (i) 3.8, (ii) 3.5, (iii) 3.0, (iv) 2.8, and (v) 2.6 Å, combined with next near distances of 3.5 Å.

363.1 K (see the Supporting Information). Interestingly, the small effect of  $C_p$  at 355 K and the turning point of the thermopower at 359 K (Figures 1 and 5) are quite consistent with this finding and must therefore be correlated to the attractive forces in the silver substructure.

The drastic changes in thermopower, electric conductivity, and thermal diffusivity have a strong influence on the thermal conductivity and the thermoelectric figure of merit (Figure 8). A pronounced peak in the thermal conductivity, consistent with the abrupt change of the silver ion mobility at the 334 K  $\beta$ - $\alpha$  phase transition, occurs. The thermal conductivity increases from very low values of  $0.19 \text{ W m}^{-1} \text{ K}^{-1}$  (329 K) before and  $0.23 \text{ W m}^{-1} \text{ K}^{-1}$  (335 K) after the transition to a maximum of  $0.60 \text{ W m}^{-1} \text{ K}^{-1}$  at 332 K. These values substantiate the effective phonon scattering process in the case of the mixed conducting  $\text{Ag}_5\text{Te}_2\text{Cl}$  over a wide range of temperature.

Thermal conductivities around  $0.2 \text{ W m}^{-1} \text{ K}^{-1}$  are usually found for elements like phosphorus ( $0.25 \text{ W m}^{-1} \text{ K}^{-1}$ ) and sulfur ( $0.27 \text{ W m}^{-1} \text{ K}^{-1}$ ) or isolators like rubber ( $0.16 \text{ W m}^{-1} \text{ K}^{-1}$ ), polyethylene ( $0.22 \text{ W m}^{-1} \text{ K}^{-1}$ ), polyvinylchloride ( $0.19 \text{ W m}^{-1} \text{ K}^{-1}$ ), or polytetrafluoroethylene.<sup>56,60–62</sup> The thermoelectric figure of merit ( $ZT$  value) performs a pronounced discontinuity at the  $\beta$ - $\alpha$  phase transition and a less pronounced one at 355 K, in good accordance with the different transitions found in independent experiments (Figure 8). Because of the jump in the total conductivity during the order/disorder phase transition, the  $ZT$  value also jumps significantly, about 2 orders of magnitude, and reaches a maximal value of 0.033 at 500 K. The absolute value is not competitive to state of the art p-type thermoelectric materials (featuring  $ZT > 1$ )<sup>7–10</sup> but the general process of a combination of electronic structure modulations and thermoelectric property tuning represents a powerful way to tune material aspects in a bulk phase.  $\text{Ag}_5\text{Te}_2\text{Cl}$  is a new p-type example (to the best of our knowledge, the second reported example within the aforementioned conceptual approach featuring attractive cation-attractions beside n-type  $\text{In}_4\text{Se}_3-\delta$ ), which follows the recently discovered concept for the improvement of thermoelectric properties based on the occurrence of low-dimensional subunits (covalent attractions and Peierls chains) in bulk materials.

#### 4. Conclusion

$\text{Ag}_5\text{Te}_2\text{Cl}$  is a mixed conductor on the quasi-binary section coinage metal chalcogenide–coinage metal halogenide featuring reversible property switches caused by  $d^{10}-d^{10}$  interactions in the solid state. An attractive interaction within the mobile silver substructure occurs

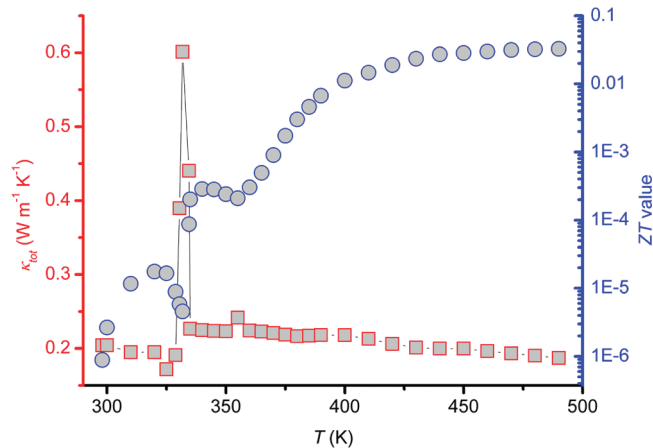


**Figure 8.** Thermal conductivity (square)  $\kappa_{\text{tot}}$  in  $\text{W m}^{-1} \text{ K}^{-1}$  and thermoelectric figure of merit  $ZT$  (circle) in the temperature range of 290–500 K. At the  $\beta$ - $\alpha$  phase transition the thermal conductivity shows a large maximum of  $0.60 \text{ W m}^{-1} \text{ K}^{-1}$  at 332 K. The  $ZT$  value performs a discontinuity at the phase transition temperature and jumps by 2 orders of magnitude during this process. At 355 K, consistent with a small maximum in  $C_p$  (see Figure 5), a second drop becomes obvious pointing toward an additional structural change in the system.

and sulfur ( $0.27 \text{ W m}^{-1} \text{ K}^{-1}$ ) or isolators like rubber ( $0.16 \text{ W m}^{-1} \text{ K}^{-1}$ ), polyethylene ( $0.22 \text{ W m}^{-1} \text{ K}^{-1}$ ), polyvinylchloride ( $0.19 \text{ W m}^{-1} \text{ K}^{-1}$ ), or polytetrafluoroethylene.<sup>56,60–62</sup> The thermoelectric figure of merit ( $ZT$  value) performs a pronounced discontinuity at the  $\beta$ - $\alpha$  phase transition and a less pronounced one at 355 K, in good accordance with the different transitions found in independent experiments (Figure 8). Because of the jump in the total conductivity during the order/disorder phase transition, the  $ZT$  value also jumps significantly, about 2 orders of magnitude, and reaches a maximal value of 0.033 at 500 K. The absolute value is not competitive to state of the art p-type thermoelectric materials (featuring  $ZT > 1$ )<sup>7–10</sup> but the general process of a combination of electronic structure modulations and thermoelectric property tuning represents a powerful way to tune material aspects in a bulk phase.  $\text{Ag}_5\text{Te}_2\text{Cl}$  is a new p-type example (to the best of our knowledge, the second reported example within the aforementioned conceptual approach featuring attractive cation-attractions beside n-type  $\text{In}_4\text{Se}_3-\delta$ ), which follows the recently discovered concept for the improvement of thermoelectric properties based on the occurrence of low-dimensional subunits (covalent attractions and Peierls chains) in bulk materials.

(60) Barbalace, K. Periodic Table of Elements—Sorted by Thermal Conductivity; <http://EnvironmentalChemistry.com/yogi/periodic/thermal.html> (1995–2010).

(61) Kalaprasad, G.; Pradeep, P.; Mathew, G.; Pavithran, C.; Thomas, S. *Compos. Sci. Technol.* **2000**, *60*, 2967.

(62) Hattori, M. *Colloid Polym. Sci.* **1964**, *1*, 11.



right after the silver order/disorder phase transition at 334 K, which results in pronounced effects in the electric and thermoelectric properties. A significant thermopower drop slightly after this phase transition temperature was observed. This finding is consistent with a recent observation and conceptional approach that a Peierls distorted arrangement of either anionic or cationic chains can cause a pronounced modulation of the electric and thermoelectric properties. In contrast to previously reported compounds following this concept which were characterized by a sharp thermopower effect, the title compound shows a plateau regime right after the thermopower drop. This plateau starts to vanish during heating because of a decreasing contribution of  $d^{10}-d^{10}$  interactions in the silver substructure. Obviously,  $\text{Ag}_5\text{Te}_2\text{Cl}$  is the second example beside  $\text{In}_4\text{Se}_{3-\delta}$  where a cationic interaction is responsible for the modulation of the physical properties. The present order/disorder phase transition is connected with huge effects in heat capacity, thermal diffusivity and conductivity. As a consequence, a strong discontinuity of the thermoelectric figure of merit develops at this temperature. A former unseen third transition was found at 355 K that is related to the reaction of the system after the

temperature-driven continuous formation of the  $d^{10}-d^{10}$  interactions and the continuous reduction of this feature with temperature afterward in the silver substructure. We have demonstrated herein that a deep investigation of attractive interactions in dynamic systems should be performed and a more detailed screening of compounds featuring high ion dynamics is needed in the future.

**Acknowledgment.** T.N. thanks the Université Bordeaux 1 for an invited professorship and the ICMCB (Institut de Chimie de la Matière Condensée de Bordeaux) for the possibility to use their facilities for thermoelectric measurements during this project. We thank Dr. M. Möller (Münster) for the assistance during the X-ray powder measurements. This project was performed within the collaborative research centre SFB 458 founded by the DFG (German Science Foundation) during the past four years.

**Supporting Information Available:** Tables and additional information concerning temperature-dependent X-ray powder and single-crystal diffraction experiments, thermal diffusivity measurements, thermal conductivity, and  $ZT$  calculations (PDF). This material is available free of charge via the Internet at <http://pubs.acs.org>.